Review Article

ATR-SEIRAS for time-resolved studies of electrode−electrolyte interfaces

Angel Cuesta[1,2]

Abstract

In this contribution, we review the application of surface-enhanced infrared spectroscopy in the attenuated total reflection mode (ATR-SEIRAS) for time-resolved studies of electrode−electrolyte interfaces. The range of time resolution reviewed goes from seconds or a fraction of a second to picoseconds, and the methodologies include fast interferometer scan rates, step-scan interferometry, frequency comb spectroscopy and pump-probe strategies. This wide range of time resolution and methodologies enables exploring the kinetics of electrochemical reactions and specific adsorption, the dynamics of double layer charging, the vibrational relaxation of adsorbates and spectral diffusion of adsorbates, all of them phenomena of the utmost importance to develop a truly deep understanding of electrode−electrolyte interfaces and electrochemical reactions.

Addresses
[1] Department of Chemistry, School of Natural and Computing Sciences, University of Aberdeen, AB24 3UE Aberdeen, Scotland, UK
[2] Centre for Energy Transition, University of Aberdeen, AB24 3FX Aberdeen, Scotland, UK

Corresponding author: Cuesta Angel (angel.cuestaciscar@abdn.ac.uk)

Introduction

Electrochemical processes are the only ones for which the theoretical efficiency with which the Gibbs free energy of a chemical reaction can be converted into useful work (or, *vice versa*, with which work can be stored in chemical bonds if $\Delta G > 0$) is 100%. It is, therefore, no wonder that so many efforts are being currently devoted to the development of the next generation of electrolysers, batteries, fuel cells and supercapacitors, all of which are expected to play key roles in our sustainable energy future and in reaching the goal of a carbon-free economy. Electrochemistry is also relevant, either by itself or as a useful set of tools, in understanding bioenergetics and electronic transport within biologically relevant molecules [1,2].

A deep knowledge of the structure and dynamics of the electrode−electrolyte interface and of the kinetics of electrochemical reactions is critical to improving the efficiency of electrochemical energy storage and conversion technologies. Since approximately the 1980s, a variety of vibrational spectroscopy techniques, like, e.g. infrared spectroscopy, Raman scattering or sum-frequency generation (SFG), and techniques capable of delivering surface structural information at the atomic level, like, e.g. scanning tunnelling microscopy (STM) or surface X-ray scattering (SXS), have been applied *in situ* to the study of electrochemical interfaces and reactions. The use of these and other non-electrochemical *in situ* techniques has resulted in a wealth of information regarding adsorbed intermediates and spectators involved in electrocatalytic reactions, their mode of bonding to the electrode surface, the structure of water or more exotic solvents at the interface, and the atomic-level structure of electrode surfaces and adsorbates, as well as how all these things depend on the applied potential. However, with some notable exceptions, most of this information corresponds to a static picture of the electrode−electrolyte interface, whereas a more dynamic description is required for a real deep understanding of electrochemical reactions and interfaces. *In-situ* spectroscopic and structural studies of electrode−electrolyte interfaces with sufficiently high time resolution remain a barely explored frontier in electrochemistry.

The time resolution required to deliver this wished-for dynamic picture of the electrode−electrolyte interface depends on the kind of process targeted. The most elemental and fastest processes, like solvent reorganization, electron tunnelling and isomerisation (which are furthermore not independent from each other), occur in time scales shorter than a nanosecond. Extremely relevant information can still be obtained from time-resolved experiments at much longer time scales, ranging from hundreds of milliseconds to nanoseconds. Because the rate of

electrochemical reactions can be changed by orders of magnitude with relatively small changes in the applied potential, the time evolution of reactants, intermediates and products can often be monitored spectroscopically with time resolutions of just some fraction of a second if sufficiently sensitive techniques are employed.

In this review, we will focus on the use of time-resolved surface-enhanced infrared spectroscopy in the attenuated total reflection mode (ATR-SEIRAS) to obtain time-resolved vibrational spectra. Due to the high sensitivity of ATR-SEIRAS, good quality spectra can often be obtained with a single interferogram, which puts the limit to the time resolution achievable on the speed with which the moving mirror of the interferometer of a Fourier-Transformed Infrared (FTIR) spectrometer can move. This can be adjusted slightly by modifying the spectral resolution (which increases with increasing distance travelled by the moving mirror) but the highest time resolutions achievable are, at best, several tens of milliseconds. This is often enough to monitor the time evolution of species involved in electrocatalytic reactions. We will show examples in which this time resolution is sufficient to provide relevant information even when dealing with much faster processes, like adsorption, and we will discuss strategies that can lead to increasing the time resolution of ATR-SEIRAS and address these faster processes in more detail. Although Zwaschka et al. [3] have recently provided an excellent review of (spectroscopic and non-spectroscopic) studies of ultra-fast processes at the electrode−electrolyte interface, we will also discuss briefly in this review the use of ATR-SEIRAS in this time domain.

Time-resolved ATR-SEIRAS for electrochemical kinetics
Electro-oxidation of small organic molecules
The high sensitivity of ATR-SEIRAS allows good quality spectra to be obtained from a single interferogram, without the need for accumulating interferograms to improve the signal-to-noise ratio. In addition, thanks to the ATR configuration, the large IR drop and transport limitations characteristic of infrared (external) reflection-absorption spectroscopy (IRRAS) are minimised, which makes ATR-SEIRAS well suited to study the kinetics of electrocatalytic reactions. In normal FTIR, the time resolution will be only limited by the speed at which the moving mirror in the interferometer can travel, i.e. by how fast a single interferogram can be collected.

Studying the adsorption and oxidation of formaldehyde on Pt with a time resolution of one spectrum per second, Jusys and Behm [4] detected for the first time adsorbed formyl from its C=O stretching band at $1635 \, \text{cm}^{-1}$. This must necessarily be the last reaction intermediate in the oxidation of formaldehyde to adsorbed CO (CO_{ad}) on Pt. Their experiments were performed using a thin-layer

spectroelectrochemical flow cell, which allows for well-controlled transport conditions but probably also leads to increased non-compensated resistance and a higher time constant of the electrochemical cell. This, however, does not affect the results reported because experiments were performed at constant potential by rapidly switching between formaldehyde-free and formaldehyde containing solutions. Unfortunately, the authors did not indicate the time needed to completely switch from the initial to the final concentration.

Jusys and Behm also observed weak broad bands at ca. 1420 and $1280 \, \text{cm}^{-1}$, which, following Batista and Iwasita [5], they tentatively assigned to the $-CH_2-$ symmetric deformation (scissoring) mode and to the C−OH stretching mode, respectively, in adsorbed methylene glycol. In aqueous solutions, H_2CO quickly establishes an equilibrium with $OH-CH_2-OH$, in which methylene glycol is the dominant species. These bands might therefore provide evidence that, as we have suggested recently [6], the oxidation of formaldehyde to CO_2 through the direct path starts with its hydrated form (methylene glycol), which is oxidised to adsorbed formate (the monodentate form of which is then oxidised to CO_2), whereas the indirect path starts with H_2CO and goes through adsorbed formyl and CO_{ad}.

Jusys and Behm [4] also obtained intensity−time profiles of the total CO_{ad} coverage (θ_{CO}) from their time-resolved experiments by using the band corresponding to linearly adsorbed CO (CO_L) as a proxy for θ_{CO} (i.e. by ignoring the contribution of bridge-bonded (CO_B) and multiply-bonded (CO_M) CO to θ_{CO}). Extrapolation to $t = 0$ allows for determining the rate constant of the dehydrogenation reaction. By performing experiments with either H_2CO or D_2CO, the kinetic isotopic effect could be determined, from which Jusys and Behm concluded that, both in the direct and indirect paths, the rds must correspond to a C−H bond breaking event.

Our group has very recently analysed the kinetics of the electrocatalytic partial oxidation of methanol to CO_{ad} on Pt [7] by monitoring current and spectral transients in methanol-containing perchloric and sulphuric acid solutions after a potential step from a potential positive enough to have a CO_{ad}-free Pt surface to a potential between 0 and 0.4 V versus RHE, where complete oxidation to CO_2 does not occur or occurs at too slow a rate to be detected. Oxidation of methanol to CO_{ad} was detected down to the most negative potential explored, namely, 0 V versus RHE [7]. We also observed a band at $1677 \, \text{cm}^{-1}$, which, following Jusys and Behm [4], was assigned to adsorbed formyl. The fact that formaldehyde and methanol share the last intermediate in their dehydrogenation to CO_{ad} suggests that, along the indirect path, methanol is first oxidised to H_2CO and then to adsorbed formyl before reaching CO_{ad}.

Another interesting observation by Pérez-Martínez et al. [7] is the existence at $E > 0.1$ V versus RHE of a delay between the first observation of the CO_B band and that of CO_L. Among other things, this implies that, at the very low coverage limit, ignoring CO_B and CO_M when using integrated band intensities to monitor the time evolution of θ_{CO} will result in an underestimation of

θ_{CO}, which is the reason for the unexpected increase in the rate of formation of CO_{ad} with increasing θ_{CO} at $t = 0$ reported by Liu et al. [8] when studying the same reaction. Pérez-Martínez et al. [7] also used their spectroscopic data to determine the Tafel slope of the reaction. As shown in Figure 1(Top), Tafel slopes of *ca.* 0.36 V $\pm$ 0.1 in 0.1 M $HClO_4$ and *ca.* 0.41 V $\pm$ 0.1 in

Figure 1
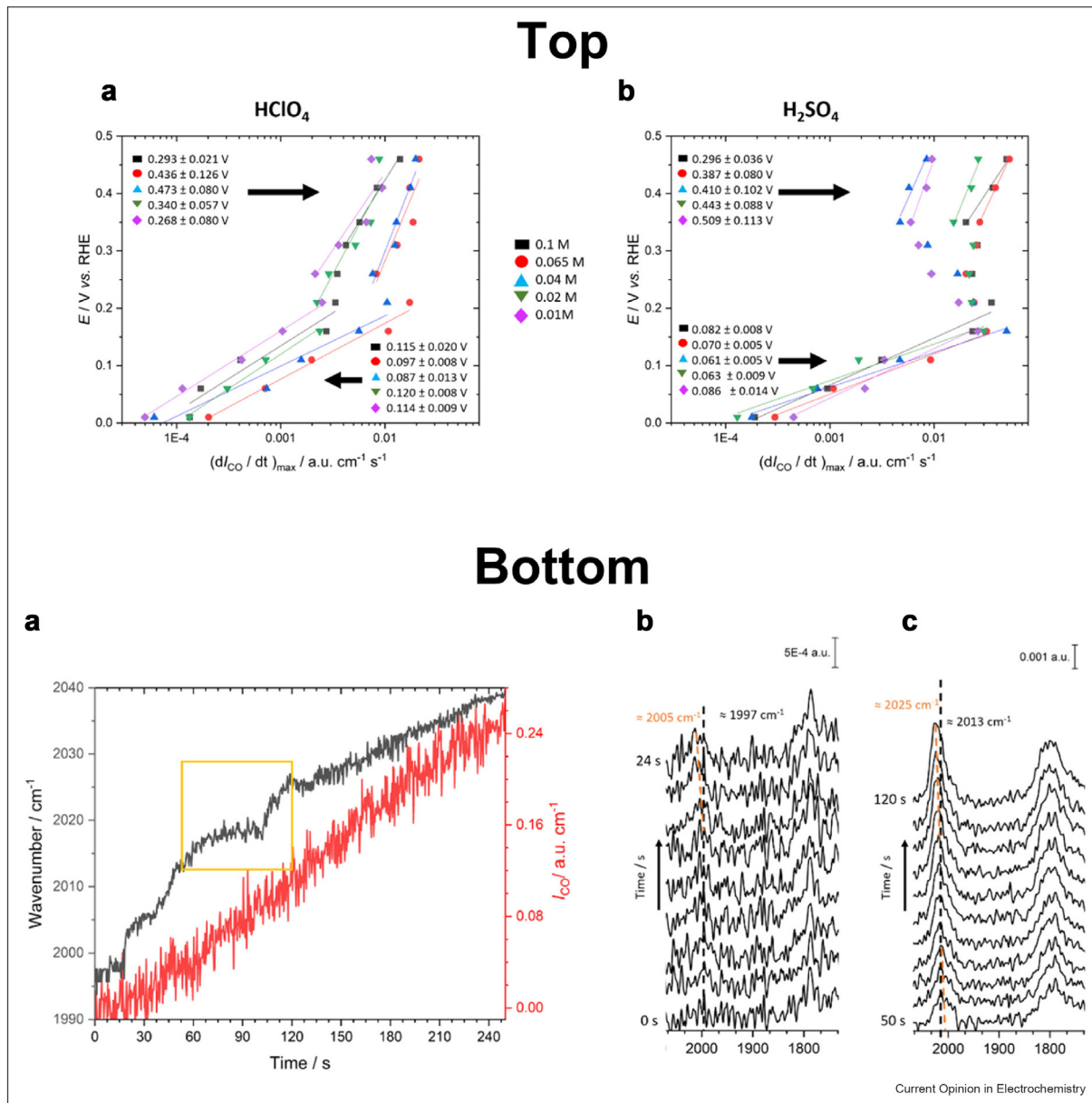
(Top) Tafel plots for the dehydrogenation of methanol to CO_{ad} on Pt in the potential region between 0.01 V and 0.46 V versus. RHE in 0.1 M $HClO_4$ (**a**) and 0.1 M H_2SO_4 (**b**) in the presence of different concentrations of methanol, as follows: 0.01 M (purple rhombi), 0.02 M (inverted green triangles), 0.04 M (blue triangles), 0.065 M (red circles), and 0.1 M (black squares). **(Bottom)** Time evolution of the stretching frequency of CO_L (black line) and of I_{CO_L} (red line) obtained from a series of time-resolved ATR-SEIRA spectra of Pt in 0.1 M H_2SO_4 containing 0.01 M CH_3OH recorded after a potential step from 0.91 to 0.06 V versus RHE (**a**). Individual spectra separated 3 s from each other and selected from the first 24 s are shown in (**b**), while spectra separated 7 s from each other and selected from the period between 50 and 120 s (yellow square in the plot on the left) are shown in the (**c**). Each spectrum consists of two interferograms recorded with a 4 cm^{-1} spectral resolution, resulting in an interval between spectra of 0.4 s. The reference spectrum was recorded at 0.91 V versus RHE. Reprinted with permission from Ref. [8]. Copyright 2021 American Chemical Society.

0.1 M H_2SO_4 were found above 0.25 and 0.35 V versus RHE, respectively, which are consistent with the Tafel slope of 0.44 ± 0.03 V obtained in 0.1 M $HClO_4$ by Liu et al. [8]. However, smaller Tafel slopes of *ca.* 0.11 V ± 0.01 and 0.07 V ± 0.01 were found by Pérez-Martínez et al. [7] in perchloric and sulfuric acid, respectively, below 0.26 V versus RHE (Figure 1(Top)), a potential region not explored by Liu et al. [8].

The most striking feature found by Pérez-Martínez et al. [7] was that at 0.21 V (0.1 M $HClO_4$) and 0.16 V (0.1 M H_2SO_4) versus RHE, the rate of the reaction stops increasing with increasingly positive potential. Instead, it remains constant, or in 0.1 M H_2SO_4, it even decreases with increasingly positive potential (Figure 1(Top, B)). This behaviour extends up to 0.26 V in 0.1 M $HClO_4$ and up to 0.36 V in 0.1 M H_2SO_4. As noted in Ref. [7], the stronger effect in 0.1 M H_2SO_4 suggests that the disruption in the expected dependence of the reaction rate on the potential is due to the adsorption of blocking spectator species, which were identified as either adsorbed OH (OH_{ad}, perchloric acid) or adsorbed sulphate ($SO_{4,ad}$, sulphuric acid).

The time-resolved experiments in Ref. [7] also allowed for the observation that, in the initial stages of the dehydrogenation of methanol to CO_{ad}, although θ_{CO} grows steadily and continuously, the CO-stretching frequency grows in a staircase manner (Figure 1(Bottom)), in which periods of constant or nearly constant frequency are followed by a sharp rise in frequency and then by a new period of constant or nearly constant frequency. This was interpreted as being due to a successive population of sites, whereby CO_{ad} diffuses from the most active sites, which are populated first, into neighbouring bidimensional domains once the CO coverage on the active defect sites reaches a threshold value.

### Kinetics of electron transfer

Tafel slopes and reaction intermediates, which together can provide useful insight into reaction mechanisms, can be spectroscopically determined and identified, respectively, with time resolutions that barely go below 1 s. However, determination of some other important kinetic parameters, like rate constants of electron transfer, requires increasing the time resolution well beyond that limit, which requires resorting to more sophisticated techniques like step-scan FTIR spectroscopy. A recent exception is the use of normal FTIR to determine the rate constant of electron transfer to a monolayer of 2,2,6,6-tetramethylpiperidine-1-oxyl [9].

To the best of our knowledge, the earliest example of an ATR-SEIRAS time-resolved step-scan FTIR study of the kinetics of an electrochemical reaction is credited to Osawa et al. [10]. Top-end research FTIR spectrometers with the step-scan mode of interferogram collection are relatively affordable. The time resolution achievable by step-scan FTIR spectroscopy is essentially limited by the sampling frequency of the detector and can easily reach some tens of microseconds. Time resolution as high as 2 ns is possible, although at the expense of losing dynamic range [11]. It might therefore appear somehow surprising that step-scan FTIR spectroscopy has not been amply used to study the dynamics of electrochemical systems. However, step-scan spectroscopy is only applicable to reversible or cyclic processes, or processes that can be repeated very reproducibly [12]. Most of the relevant electrocatalytic reactions do not fulfil these conditions and are, therefore, not well suited for step-scan spectroscopy. A scheme describing the mode of operation of step-scan time-resolved FTIR spectroscopy when the spectrometer triggers the excitation of the system (in the case of electrochemical problems, typically, but not necessarily, through a potential step) is provided in Figure 2.

Nauman and co-workers have intensely studied the kinetics of electron transfer of cytochrome c [13] and cytochrome c oxidase [14−16]. An important feature of their work is the use of phase-sensitive detection (PSD) to improve the signal-to-noise ratio [16]. This was achieved by applying an algorithm to the time-resolved step-scan spectra recorded while a square wave is applied to the electrode potential. Control of the frequency of the square wave allows for choosing the bands whose signal to noise ratio is to be improved [13], which allowed them to monitor the kinetics of electron transfer with time resolution down to 50 μs. An alternative way to determine rate constants of electron transfer processes by applying (PSD) coupled with step-scan FTIR is to analyse the frequency dependence of the in-phase and out-of-phase components of the potential-modulated IR spectrum as demonstrated by Ataka et al. [17]. In this case, step-scan is not used to obtain time-resolved spectra; instead, the frequency-dependent potential-modulated spectrum is reconstructed from the frequency-dependent response of the detector signal to the potential modulation at each position of the moving mirror. The analysis of complex-plane plots of the optical impedance obtained from in-phase and out-of-phase spectra at frequencies between 40 Hz and 100 kHz (please see Ref. [17] for a definition of optical impedance and its calculation) allows for determining the Faradaic resistance. Using this method, Ataka et al. identified a charge transfer process between the gold surface and adsorbed 4-mercaptopyridine (PySH) in Au electrodes modified with a PySH self-assembled monolayer and were able to determine the rate constant of the charge-transfer process (5.4×10^5 s^{-1}).

Figure 2
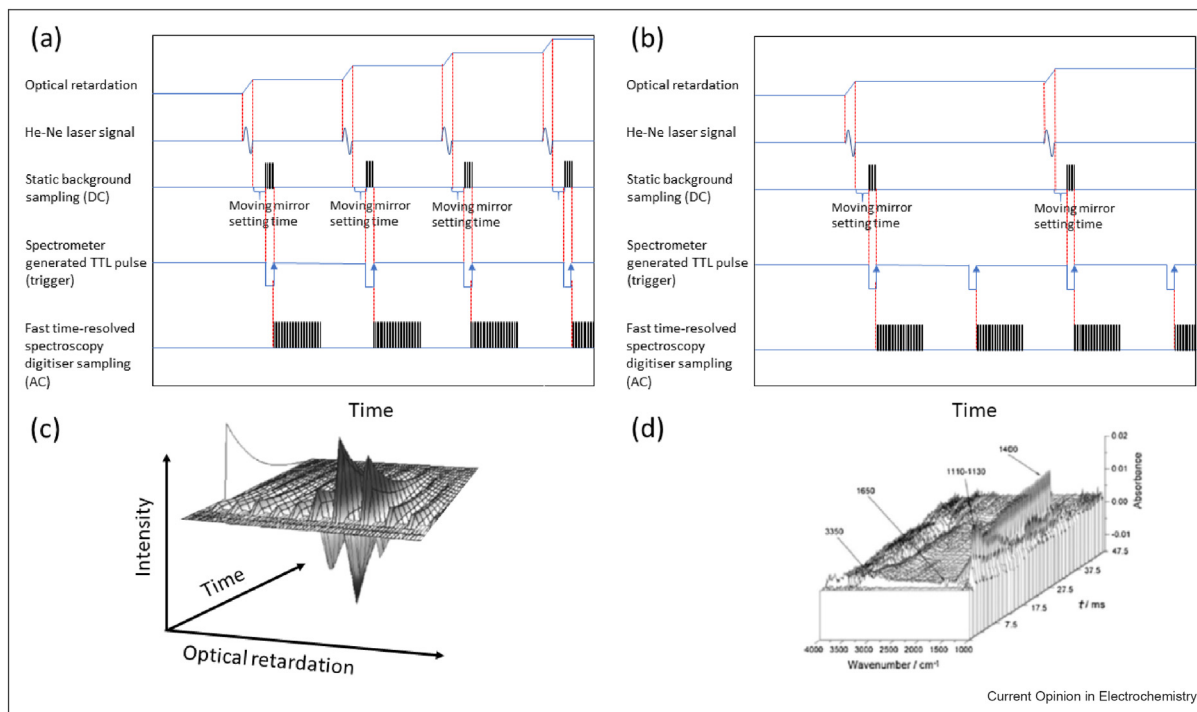
Scheme describing the mode of operation of step-scan time-resolved FTIR spectroscopy. **(a)** and **(b)** show the time sequence for experiments with a single and with two triggers per mirror step, respectively. A typical experiment involves the following steps: (i) The moving mirror steps to the first position and then holds stationary during the experimenter-determined *Settling Time*; (ii) Data points are collected from the DC output of the detector preamplifier over the experimenter-determined *Static Average Time* and used later to build the static interferogram; (iii) A synchronised TTL pulse generated by the spectrometer triggers the external excitation source (e.g. a potentiostat or waveform generator) that initiates the time-dependent process; (iv) Changes in spectral intensity are recorded from the AC output of the detector preamplifier over a period and at intervals set by the user. When several trigger events occur per mirror step, the data collected after each trigger are averaged to improve the signal-to-noise ratio, which is equivalent to recording several interferograms in the normal FTIR operation mode; (v) The moving mirror moves to the next position and steps (i) to (iv) are repeated; (iv) Interferograms at the preselected time intervals are reconstructed from the time-dependent points recorded at each mirror position **(c)**, which can then be Fourier-transformed to a set of time-dependent spectra (**d**, Reprinted with permission from Ref. [13]. Copyright 2008 Elsevier).

ATR-SEIRAS monitoring of adsorption and double-layer dynamics

Adsorption processes and double-layer dynamics are intrinsically fast processes (please note that double-layer rearrangement after a perturbation, e.g., a potential step, can be relatively slow, but this will be determined by the cell's time constant, not by the double-layer dynamics itself). Their study, therefore, requires pushing the time resolution into the sub-millisecond regime and beyond. This is not a big problem in the case of specific adsorption of ions and double-layer charging, which are usually very reversible processes and can therefore be studied using step-scan FTIR, which is unfortunately much more difficult to implement in the case of irreversible adsorption processes.

That said, useful insight into irreversible adsorption processes can be obtained with lower time resolution if the adsorption process is slowed down by carefully controlling the dosing of the adsorbate. An example of this strategy has been provided by Silva et al. [18], who

were able to monitor using ATR-SEIRAS the adsorption of CO on a Pt electrode during potentiostatic CO-charge displacement experiments in 0.1 M H_2SO_4. The experiments revealed that when CO is adsorbed directly from the solution, CO_L is preferred to CO_B/CO_M sites, and is occupied first. It is worth noting here that this behaviour is interestingly not reproduced when CO_{ad} is formed by partial oxidation of methanol [7], in which case, and depending on the applied potential, as much as 6−8 s can elapse between the first observation of CO_B/CO_M and that of CO_L (Figure 2(A)). During the initial stages of adsorption, when θ_{CO} is very low, the absence of dipole−dipole coupling allows distinguishing between CO_L adsorbed on (100)-like defect sites (lower frequency CO_L band) and (110)- like defect + (111) terrace sites (higher frequency CO_L band). The CO_L band at higher frequencies was found to appear first, suggesting adsorption on (110)-like defect sites is slightly favoured over adsorption on (100)-like defect sites. The analysis of the evolution of the bands in the regions of the ν(OH) and δ(HOH) vibrational modes of

water revealed that the essentially hydrogen bond-free water layer characteristic of water adsorbed on CO-covered Pt only appears when a relatively high CO coverage has been reached, and therefore, requires relatively compact CO_{ad} islands.

Berná et al. [19] have provided one of the very few examples of the combination of step-scan FTIR spectroscopy and ATR-SEIRAS to study the dynamics of reversible adsorption processes at the electrode −electrolyte interfaces. Other examples preceding Berná et al.'s work are: (i) Osawa and co-workers's studies of the adsorption of fumaric acid [20] and p-nitrobenzoic acid [21], as well as of the desorption of sulphate accompanying the dissolution of the $\sqrt{3} \times \sqrt{3}$ under-potentially deposited Cu layer (Cu upd) on evaporated quasi-Au(111) electrodes [22], (ii) Wandlowski and co-workers' studies of the adsorption of trimesic acid [23] and uracil [24], also on evaporated quasi-Au(111) films, and (iii) Rodes et al.'s study of the adsorption of sulphate on silver electrodes [25]. Recently, Nakamura et al. [26] have monitored the initial stages of the underpotential deposition (upd) of Tl^+, Ag^+, Cu^{2+}, Zn^{2+}, Cd^{2+}, and Bi^{3+} on Au(111) using time-resolved surface x-ray diffraction and, in the case of Cu^{2+}, also ATR-SEIRAS combined with step-scan FTIR.

Berná et al.'s work focused on the specific adsorption of acetate on Au. Their time-resolved step-scan ATR-

SEIRA spectra (Figure 3, left) were collected after a potential step in 0.1 M $HClO_4$ solutions containing different concentrations of sodium acetate. A quantitative analysis of the time-dependent intensity of the infrared bands (Figure 3, right) showed that adsorption fits Langmuir kinetics, which suggests random adsorption of acetate anions with no preference for specific sites. The step-scan ATR-SEIRA spectra in acetate-free solutions also revealed transient strongly hydrogen-bonded water structures that decay as perchlorate adsorption proceeds after a potential step (Figure 3, left (A)). Similar bands appeared in the acetate-containing solutions, albeit with much lower intensity (Figure 3, left (B)). This is evidence of the ability of step-scan ATR-SEIRAS to monitor the different stages through which the structure of interfacial water transits during double-layer charging after a potential step, a topic which, to the best of our knowledge, has not been explored at all.

Very recently, Morhart et al.' [27] have studied the desorption of a monolayer of 4-mehoxipyridine using a microband electrode. The microsecond time domain explored by Morhart et al. [27] is particularly important because, due to limitations imposed by double-layer charging, as well as by the response time of potentiostats, it is the limit that can be achieved by potential step methods. Reaching this regime requires decreasing the electrochemical cell's time constant down to just a

Figure 3
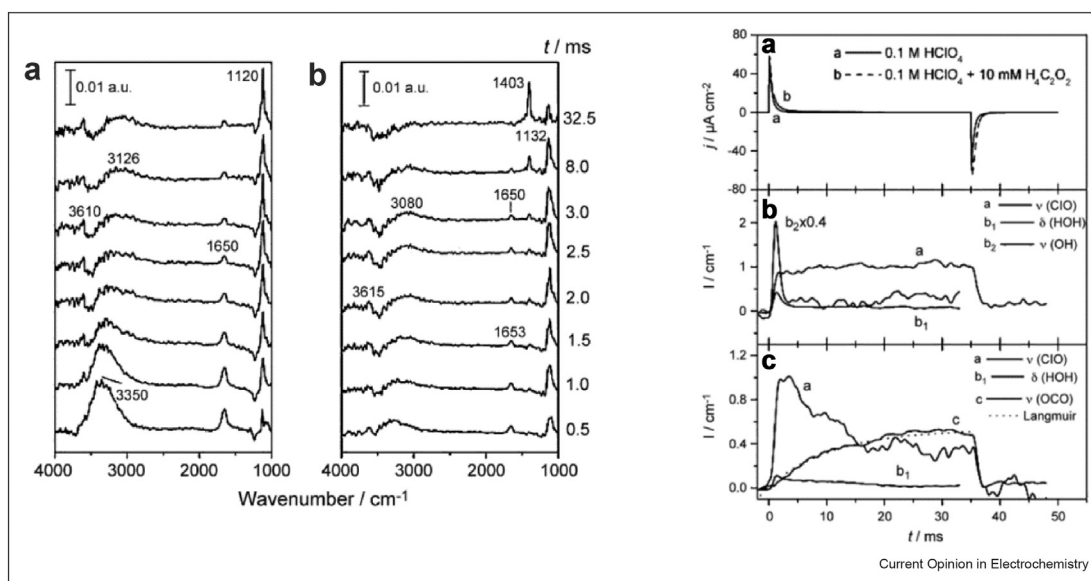
Left: Selected step-scan spectra obtained in a potential-step experiment from 0.50 to 1.10 V versus RHE in **(a)** 0.1 M $HClO_4$ and **(b)** 0.01 M CH_3COONa + 0.1 M $HClO_4$. The reference spectrum was collected at 0.50 V just before the potential step. **Right: (a)** Current density transients measured after a potential step from 0.20 to 1.10 V versus RHE and back in **(a)** 0.1 M $HClO_4$ and **(b)** 0.01 M CH_3COONa + 0.1 M $HClO_4$. **(b, c)** Time-dependent integrated intensities of the infrared bands corresponding to perchlorate **(a)**, water **(b)** and acetate **(c)** obtained from step-scan spectra recorded during the potential step in 0.1 M $HClO_4$ **(b)** and **(c)** 0.01 M CH_3COONa + 0.1 M $HClO_4$. Reprinted with permission from Ref. [13]. Copyright 2008 Elsevier.

few microseconds, which Morhart et al. achieved by depositing a gold microband electrode on an indium tin oxide (ITO) modified Si groove, which was used as the ATR substrate. They used synchrotron radiation in an attempt to improve the signal-to-noise ratio (which would be high with a conventional IR source due to the low number of photons internally reflected from the micro-sized electrode−electrolyte interface). However, this led to an unexpectedly high level of noise at low frequencies due to electromagnetic coupling of the mains frequency to a variety of mechanical devices running on the experimental floor of the synchrotron facility. The same group have also been the first to report the use of dual-frequency comb IR spectroscopy in combination with ATR-SEIRAS to monitor the dynamics of the electrode−electrolyte interface with time resolution in the microsecond domain [28]. They monitored the potential-induced desorption of 4-dimethylaminopyridine from a gold nanoparticle film electrode deposited on an ITO-modified Si prism and demonstrated the ability of dual-frequency comb IR spectroscopy to achieve time resolution in the microsecond regime (Figure 4(A)), requiring less time for data acquisition than step-scan spectroscopy. The level of noise (Figure 4(B)) was lower than in the experiments using synchrotron radiation [27] which, together with the high photon flux characteristic of laser pulses, opens interesting possibilities in terms of combining dual-frequency combs with microband electrodes. One drawback, however, is the narrow spectral window inherent to the frequency comb method.

Pump-probe strategies

While step-scan FTIR or frequency-comb methods combined with potential-step experiments allow increasing the time resolution into the sub-millisecond regime down to the microsecond time domain, going beyond this threshold down to the picosecond regime requires more sophisticated strategies. Zwaschka et al. [3] and Kraack and Hamm [29] have recently published excellent reviews of methods to characterise ultrafast processes at electrode−electrolyte interfaces, and we will not examine them in-depth here, but we think it convenient to re-examine here the ultrafast ATR-SEIRAS-based methods.

In a series of articles, Yamakata et al. [30−32] have demonstrated that recording ATR-SEIRA spectra using adequately delayed short infrared pulses after a laser-induced temperature jump at the electrode−electrolyte interface allows to cover the range of time resolution from microsecond to picosecond. It is worth mentioning that, although the response to the perturbation is not limited in these experiments by the cell's time constant, they are still limited by how fast the interface heats and dissipates energy after the heating laser pulse. Time resolution is obviously limited by the duration of the laser pulses. Using the CO stretching frequency as a probe of the interfacial potential, Yamakata et al. [30] were able to monitor coulostatic potential transients after a laser-induced temperature jump peaking at around 200 ps, which cannot be achieved if conventional electrochemical methods are used.

Figure 4
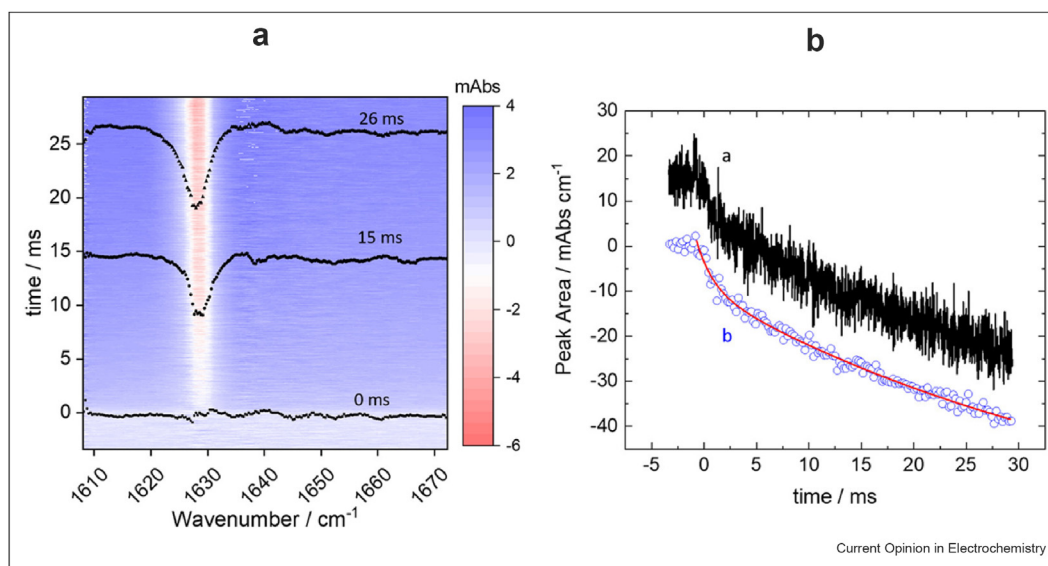
Time-resolved evolution of the ATR-SEIRAS absorbance change **(a)** during the desorption of 4-dimethylaminopyridine after a potential jump from +0.30 to −0.90 V, obtained using dual-frequency comb IR spectroscopy and time evolution of the integrated peak area of the A' ring mode of 4-dimethylaminopyridine at 1628 cm^{-1} **(b)** using (a) 20 μs and (b) 200 μs time binning. The red line is a fit to a double exponential decay. Reprinted with permission from Ref. [26]. Copyright 2020 American Chemical Society.

Kraack et al. [33] have investigated the surface enhancement effect in pump-probe 2D ATR-SEIRAS. Classical ATR-SEIRAS requires metal films deposited on the infrared-transparent substrate with a thickness above the percolation threshold to avoid too large a resistance within the thin metal film, which would lead to too large IR drops [34]. In the case of pump-probe 2D ATR-SEIRAS, however, the film resistance is not an issue because perturbing the system does not involve a potential step but a pump laser pulse. Much thinner films below 1 nm can be therefore used, which are also closer to the conditions under which the SEIRA effect is maximum, often at the expense of anti-absorption or bipolar bands [35,36]. Using their pump-probe 2D ATR-SEIRAS technique, this group has been able to measure the vibrational relaxation time constant of CO adsorbed on Pt nanoparticles deposited on an indium tin oxide (ITO) electrode. A very mildly potential-dependent time constant of 2.5 ± 0.1 ps at -1.0 V and 3.1 ± 0.1 ps at 0.4 V versus Ag/AgCl (KCl_{sat}) was found [37]. Spectral diffusion dynamics, which is determined by the interaction between adsorbed CO and the surrounding interfacial water molecules, was also investigated and was found to also depend very little on the applied potential [37]. This was attributed to (i) the lack of significant potential-dependent alignment or ordering of adsorbed molecules with respect to the surface and (ii) too weak an influence of the applied electric field on the reorientation and hydrogen bonding of water molecules in close proximity to the surface on the intermolecular dynamics due to the kind of electrode material used (Pt nanoparticles deposited on ITO).

Conclusions and outlook

Due to its high sensitivity, ATR-SEIRAS is well suited for time-resolved vibrational spectroscopy studies of electrode–electrolyte interfaces. Most importantly, the time resolution achievable by combining ATR-SEIRAS with other experimental methodologies covers the whole range from the second/sub-second range to the picosecond regime, which allows exploring a whole variety of parameters and phenomena of physical and chemical relevance. These include the kinetics and mechanisms of electrocatalytic reactions, the dynamics of adsorption and double layer charging, vibrational relaxation, and vibrational diffusion due to intra-molecular and/or intermolecular interactions.

Given the huge range of time resolution available and the relevance of the phenomena that can be explored in each of the accessible time scales, it is indeed surprising that the number of time-resolved experiments that have been reported to date is rather small (see the relatively short bibliographical list spanning a very long period of time). It is particularly worth highlighting the scarcity of studies making use of step-scan FTIR spectroscopy and pump-probe methods, which are well established in other fields. It is true that electrochemical systems involve particularly challenging experimental conditions, but the field should be sufficiently mature to explore the potential of these powerful tools.

Declaration of competing interest

The authors declare that they have no known competing financial interests or personal relationships that could have appeared to influence the work reported in this paper.

References

Papers of particular interest, published within the period of review, have been highlighted as:

* of special interest
** of outstanding interest

1. Artés JM, Díez-Pérez I, Gorostiza P: **Transistor-like behavior of single metalloprotein junctions**. *Nano Lett* 2012, **12**: 2679–2684.

2. Ruiz MP, Aragonès AC, Camarero N, Vilhena JG, Ortega M, Zotti LA, Pérez R, Cuevas JC, Gorostiza P, Díez-Pérez I: **Bioengineering a single-protein junction**. *J Am Chem Soc* 2017, **139**:15337–15346.

3. Zwaschka G, Lapointe F, Campen RK, Tong Y: **Characterization of ultrafast processes at metal/solution interfaces: towards femtoelectrochemistry**. *Curr Opin Electrochem* 2021, **29**: 100813.

4. * Jusys Z, Behm RJ: **Adsorption and oxidation of formaldehyde on a polycrystalline Pt film electrode: an in situ IR spectroscopy search for adsorbed reaction intermediates**. *Beilstein J Nanotechnol* 2014, **5**:747–759.
    A detailed time-resolved study of the adsorption and oxidation of formaldehyde on Pt using an electrochemical flow cell that enables for rapid exchange of the electrolyte in contact with the electrode surface. First report of the detection of adsorbed formyl as the last intermediate in the formation of adsorbed CO.

5. Batista EA, Iwasita T: **Adsorbed intermediates of formaldehyde oxidation and their role in the reaction mechanism**. *Langmuir* 2006, **22**:7912–7916.

6. Cuesta A: **Electro-oxidation of C1 organic molecules on Pt electrodes**. *Curr Opin Electrochem* 2017, **4**:32–38.

7. * Pérez-Martínez L, Machado de los Toyos LM, Shibuya JJT, Cuesta A: **Methanol dehydrogenation on Pt electrodes: active sites and role of adsorbed spectators revealed through time-resolved ATR-SEIRAS**. *ACS Catal* 2021, **11**:13483–13495.
    Very detailed time-resolved study of the kinetics of the partial oxidation of methanol to adsorbed CO. It includes the determination of the Tafel slope in a wide potential range, the monitoring of the sequential occupation of reaction sites and the confirmation of adsorbed formyl as the last reaction intermediate before adsorbed CO.

8. Liu SX, Liao LW, Tao Q, Chen YX, Ye S: **The kinetics of CO pathway in methanol oxidation at Pt electrodes, a quantitative study by ATR-FTIR spectroscopy**. *Phys Chem Chem Phys* 2011, **13**:9725–9735.

9. Unni B, Burgess IJ: **Electrochemical and surface enhanced infrared absorption spectroscopy studies of TEMPO self-assembled monolayers**. *Electrochim Acta* 2021, **381**:138263.

10. Osawa M, Yoshii K, ichi Ataka K, Yotsuyanagi T: **Real-time monitoring of electrochemical dynamics by submillisecond time-resolved surface-enhanced infrared attenuated-total-reflection spectroscopy**. *Langmuir* 1994, **10**:640–642.

11. Jiang EY: *Advanced FT-IR spectroscopy*. Madison, WI, USA: Thermo Fisher Scientific Inc.; 2007.

12. Rammelsberg R, Boulas S, Chorongiewski H, Gerwert K: **Set-up for time-resolved step-scan FTIR spectroscopy of noncyclic reactions**. *Vib Spectrosc* 1999, **19**:143−149.

13. Nowak C, Luening C, Schach D, Baurecht D, Knoll W, Naumann RLC: **Electron transfer kinetics of cytochrome C in the submillisecond time regime using time-resolved surface-enhanced infrared absorption spectroscopy**. *J Phys Chem C* 2009, **113**:2256−2262.

14. Steininger C, Reiner-Rozman C, Schwaighofer A, Knoll W, Naumann RLC: **Kinetics of cytochrome c oxidase from R. sphaeroides initiated by direct electron transfer followed by tr-SEIRAS**. *Bioelectrochemistry* 2016, **112**:1−8.

15. Schwaighofer A, Steininger C, Hildenbrandt DM, Srajer J, Nowak C, Knoll W, Naumann RLC: **Time-resolved surface-enhanced IR-absorption spectroscopy of direct electron transfer to cytochrome c oxidase from R. Sphaeroides**. *Biophys J* 2013, **105**:2706−2713.

16. Schwaighofer A, Ferguson-Miller S, Naumann RLC, Knoll W, Nowak C: **Phase-sensitive detection in modulation excitation spectroscopy applied to potential induced electron transfer in cytochrome c oxidase**. *Appl Spectrosc* 2014, **68**:5−13.

17. Ataka K, Hara Y, Osawa M: **A new approach to electrode kinetics and dynamics by potential modulated Fourier transform infrared spectroscopy**. *J Electroanal Chem* 1999, **473**:34−42.

18. Silva CD, Cabello G, Christinelli WA, Pereira EC, Cuesta A: **Simultaneous time-resolved ATR-SEIRAS and CO-charge displacement experiments: the dynamics of CO adsorption on polycrystalline Pt**. *J Electroanal Chem* 2017, **800**:25−31.

19. Berná A, Delgado JM, Orts JM, Rodes A, Feliu JM: **Spec-
* troelectrochemical study of the adsorption of acetate anions at gold single crystal and thin-film electrodes**. *Electrochim Acta* 2008, **53**:2309−2321.
Excellent example of the application of step-scan FTIR spectroscopy to study the reversible adsorption at the electrode-electrolyte interface.

20. Noda H, Ataka K, Wan LJ, Osawa M: **Time-resolved surface-enhanced infra-red study of molecular adsorption at the electrochemical interface**. *Surf Sci* 1999, **427−428**:190−194.

21. Noda H, Wan LJ, Osawa M: **Dynamics of adsorption and phase formation of p-nitrobenzoic acid at Au(111) surface in solution: a combined surface-enhanced infrared and STM study**. *Phys Chem Chem Phys* 2001, **3**:3336−3342.

22. Ataka K, Nishina G, Cai W-B, Sun S-G, Osawa M: **Dynamics of the dissolution of an underpotentially deposited Cu layer on Au(111): a combined time-resolved surface-enhanced infrared and chronoamperometric study**. *Electrochem Commun* 2000, **2**:417−421.

23. Han B, Li Z, Pronkin S, Wandlowski T: **In situ ATR-SEIRAS study of adsorption and phase formation of trimesic acid on Au(111-25 nm) film electrodes**. *Can J Chem* 2011, **82**:1481−1494.

24. Pronkin S, Wandlowski T: **Time-resolved in situ ATR-SEIRAS study of adsorption and 2D phase formation of uracil on gold electrodes**. *J Electroanal Chem* 2003, **550−551**:131−147.

25. Rodes A, Orts JM, Pérez JM, Feliu JM, Aldaz A: **Sulphate adsorption at chemically deposited silver thin film electrodes: time-dependent behaviour as studied by internal reflection step-scan infrared spectroscopy**. *Electrochem Commun* 2003, **5**:56−60.

26. Nakamura M, Banzai T, Maehata Y, Endo O, Tajiri H, Sakata O, Hoshi N: **Real−time observation of interfacial ions during electrocrystallization**. *Sci Rep* 2017, **71**(2017):1−9.

27. Morhart TA, Tu K, Read ST, Rosendahl SM, Wells G, Achenbach S, Burgess IJ: **Surface enhanced infrared spectroelectrochemistry using a microband electrode**. *Can J Chem* 2021:1−5.

28. Lins E, Read S, Unni B, Rosendahl SM, Burgess IJ: **Microsecond
** resolved infrared spectroelectrochemistry using dual frequency comb IR lasers**. *Anal Chem* 2020, **92**:6241−6244.
First example of the use of dual-frequency comb spectroscopy to obtain time-resolved ATR-SEIRA spectra in the microsecond time domain.

29. Kraack JP, Hamm P: **Surface-sensitive and surface-specific ultrafast two-dimensional vibrational spectroscopy**. *Chem Rev* 2016, **117**:10623−10664.

30. Yamakata A, Uchida T, Kubota J, Osawa M: **Laser-induced potential jump at the electrochemical interface probed by picosecond time-resolved surface-enhanced infrared absorption spectroscopy**. *J Phys Chem B* 2006, **110**:6423−6427.

31. Yamakata A, Osawa M: **Dynamics of double-layer restructuring on a platinum electrode covered by CO: laser-induced potential transient measurement**. *J Phys Chem C* 2008, **112**:11427−11432.

32. Yamakata A, Osawa M: **Cation-dependent restructure of the electric double layer on CO-covered Pt electrodes: difference between hydrophilic and hydrophobic cations**. *J Electroanal Chem* 2017, **800**:19−24.

33. Kraack JP, Kaech A, Hamm P: **Surface enhancement in ultrafast 2D ATR IR spectroscopy at the metal-liquid interface**. *J Phys Chem C* 2016, **120**:3350−3359.

34. Osawa M, Ataka K, Yoshii K, Yotsuyanagi T: **Surface-enhanced infrared ATR spectroscopy for in situ studies of electrode/electrolyte interfaces**. *J Electron Spectrosc Relat Phenom* 1993, **64−65**:371−379.

35. Pecharromán C, Cuesta A, Gutiérrez C: **Calculation of adsorption-induced differential external reflectance infrared spectra of particulate metals deposited on a substrate**. *J Electroanal Chem* 2004, **563**:91−109.

36. Pecharromán C, Cuesta A, Gutiérrez C: **Comments on the paper by M.-S. Zheng and S.-G. Sun entitled 'In situ FTIR spectroscopic studies of CO adsorption on electrodes with nanometer-scale thin films of ruthenium in sulfuric acid solutions' [J. Electroanal. Chem. 500 (2001) 223]**. *J Electroanal Chem* 2002, **529**:145−154.

37. Lotti D, Hamm P, Kraack JP: **Surface-sensitive spectro-
** electrochemistry using ultrafast 2D ATR IR spectroscopy**. *J Phys Chem C* 2016, **120**:2883−2892.
Excellent example of the use of pump-probe spectroscopic methods to investigate extremely fats interfacial processes, like vibrational relaxation and dissipation of vibrational energy through intermolecular and intramolecular interaction.